ARMY RESEARCH LABORATORY

Measurement of Viscosity of Reacting Vinyl-Ester Resins Using Direct-Current Sensing

by Bruce K. Fink, Kenric M. England,
and John W. Gillespie Jr.

ARL-TR-2149 January 2000

The findings in this report are not to be construed as an official Department of the Army position unless so designated by other authorized documents.

Citation of manufacturer's or trade names does not constitute an official endorsement or approval of the use thereof.

Destroy this report when it is no longer needed. Do not return it to the originator.

Abstract

This study investigated the sensing of viscosity an gelation of reacting vinyl-ester (VE) resins using direct-current (DC) sensing technology. The resin system studied was a tetrabutylammonium acetate (TA)-doped Dow Derakane 411-C-50 VE resin. A model of the resistance of a reacting polymer liquid as a function of the geometrical parameters of the DC-sensing system and the material properties of the resin system was developed. The model inputs were conduction path length (L), conductor surface area (A), resin viscosity ($\eta(t)$), concentration of TA ions (C_i), charge of TA ions (Q_i), and size of TA ions. Estimates, using the theoretically determined values for the model inputs, for the resistance of the DC sensing system employed in this investigation were the same order of magnitude as the experimentally determined values. The developed model of a reacting polymer liquid was further extended to the sensing of gelation and then successfully applied to the on-line sensing of viscosity.

Table of Contents

INTENTIONALLY LEFT BLANK.

List of Figures

INTENTIONALLY LEFT BLANK.

1. Introduction

As the composites industry grows, there is an increasing need to improve quality and reduce the cost of producing composite structures. To meet these demands, industry has begun to develop and refine new technologies to monitor the condition of a composite during manufacturing. A technique currently under development at the U.S. Army Research Laboratory (ARL) is sensors mounted as roving threads (SMARTweave), a patented sensor system that monitors the direct-current (DC) conductance of a resin as it flows into a resin transfer molding (RTM) mold and cures [1–6]. This is done through an overlapping, but not touching, grid of wires; one set serves as excitation leads, and an orthogonal set in a parallel plane serves as sensing leads. The resin acts as a resistor and, under an applied voltage, current is induced in a circuit containing the resin gap resistor.

One common approach in single-point flow and cure sensing is to monitor the dielectric response of a material by the application of an alternating current. However, such techniques track not only the ionic conductivity of the curing resin but a more complex dielectric response as well. The use of a DC measurement technique allows for a simpler measurement of DC conductance for rapid continuous multiplexing of potentially thousands of "point sensors" in a mold.

Many resin systems, such as vinyl esters (VEs), commonly used in composite manufacturing have an inherently high resistivity. VE resin systems have a wide range of commercial applications and are used in composite structures such as bridge supports, railroad cars, and diesel busses. VE resin systems are easy to process as a result of their low viscosity and adjustable gel times, making them amenable to composite liquid-molding processes. Resin, initiator, and accelerator chemistry control the viscosity and gel times of VE resins.

In this report, a model is developed that will predict the relationship between resistance and material properties such as viscosity, concentration of ions, and SMARTweave geometrical parameters. The resin system that is investigated is a Dow Derakane 411-C-50 VE resin system.

An organic salt, tetrabutylammonium acetate (TA), has been added to the resin to optimize DC sensing and produce a more controlled ionic conductivity for the purpose of linking the response of DC conductivity measurement systems such as SMARTweave to more important characteristics of the curing process such as viscosity, time to gel, and time to cure [6]. The model inputs are characterized through the use of SMARTweave single-node test cells (SNTC) in combination with viscometry and differential scanning calorimetry (DSC). The culmination of these studies is the integration of a DC-sensing system and a ionic conductivity model that can provide real-time information about the viscosity and onset of gelation during the cure of VE resin systems.

2. Background and Theory

Two parameters govern the operation of DC-sensing systems: (1) the geometric configuration of the sensing system and (2) the material properties of the resin system. The geometric parameters of interest are conductor separation distance and surface area. The material properties of interest are viscosity, concentration of ions, and size of ions. Both the viscosity of the transporting medium and ionic radius influence ionic mobility.

Figure 1 shows the chemical structure and makeup of the VE and styrene monomers. A cobalt napthenate (CoNap) accelerator is used along with a cumene hydroperoxide-based catalyst, Trigonox 239A. The system is mixed with 2.0 weight-percent (wt-%) Trigonox 239A and 0.2 wt-% CoNap, then allowed to cure at room temperature.

The polymerization of VE and styrene resin occurs by a free radical polymerization reaction. Free radical polymerization, or chain polymerization, is characterized by the growth of a polymer chain in which only one repeating unit is added to the chain at a time. In the first stage of chain polymerization of VEs, an organic peroxide or hydroperoxide, called an initiator, attacks the vinyl group in the VE and generates a free radical. For a low-temperature cure, an accelerator, such as CoNap, is used to lower the free-energy barrier to free radical generation. Free radicals generated by the initiator then bond with other free radicals, either those adjoined to

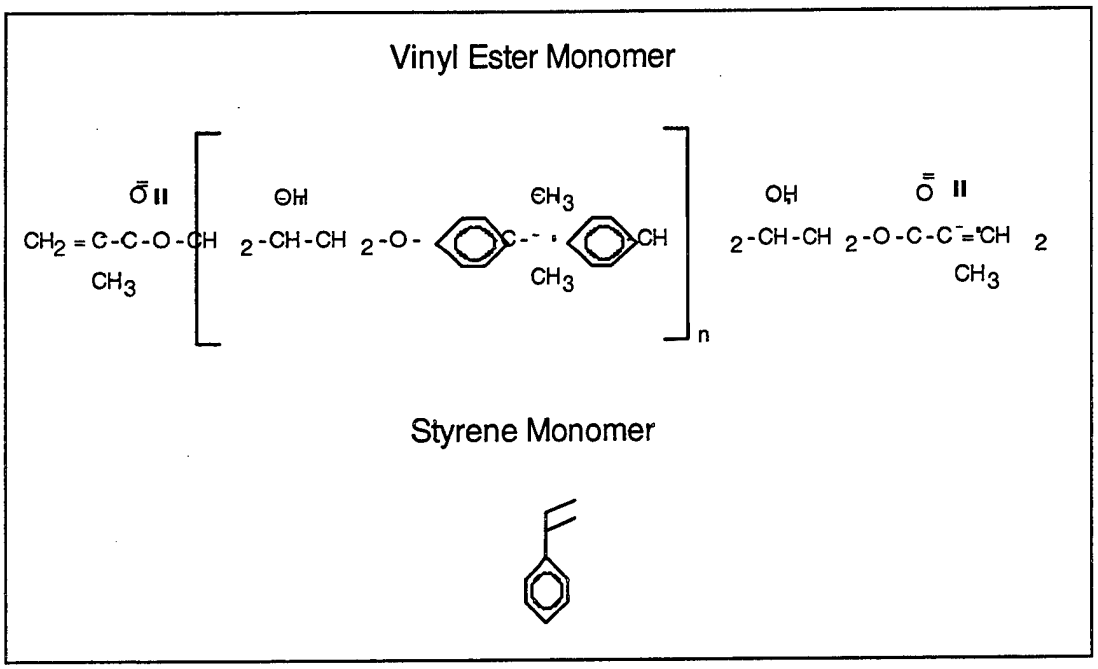

Figure 1. VE and Styrene Monomer Structures and Chemical Makeup.

other VE functional sites or to styrene monomers. The repeated generation of free radicals and subsequent bonding of adjacent free radicals is called cross-linking.

A fairly rapid increase in viscosity characterizes the initial stages of chain polymerization reaction. The point at which viscosity tends toward infinity is gelation and is characterized by a cross-linked VE and styrene network, swollen with unreacted monomers. As the reaction proceeds, further incorporation of monomers in the polymer network is controlled more by diffusional mobility of monomers than by reaction kinetics. Vitrification is the point at which monomers are unable to diffuse to active sites along the polymer chain, and the material becomes glassy in nature, or vitrified.

In a related study, the ionic conductivity of different dopants for VE resin were characterized [6]. The addition of dopants such as TA were found to provide consistent concentrations with minimal effects on viscosity, degree of conversion, and gelation times. Figure 2 shows the chemical structures of tetrabutylammonium and acetate ions. The hydrodynamic radius of tetrabutylammonium and acetate ions has been calculated to be 5.5 and 3.75 Å, respectively [6].

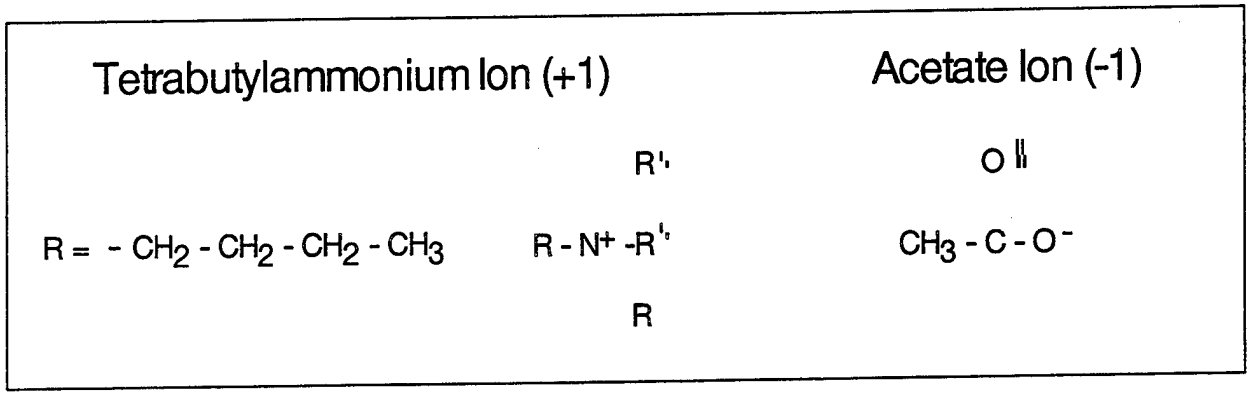

Figure 2. Tetrabutylammonium and Acetate Ions.

A model to predict the resistance of a liquid resin based on the geometric parameters of the sensing system and on the properties of the resin was previously developed by Schwab, Levy, and Glover [7]. The model is based on the balance between the electrostatic force felt by an ion being acted upon by an applied potential difference and the viscous drag force that the ion encounters as it tries to move through a viscous medium. Equation (1) is the result of such a balance of forces:

$$R_j(t) = \frac{6\pi\eta(t)L}{A\sum_i \frac{C_i Q_i^2}{r_i}}. \tag{1}$$

The resistance, $R_j(t)$, is the resin resistance at a SMARTweave sensor junction, $\eta(t)$ is viscosity at time (t) in Pascal-seconds, L is the conductor separation distance in meters, A is area of the effective DC electric field in square meters, C_i is the concentration of the ith ion in ions per cubic meter, Q_i is the charge of the ith ion in coulombs, and r_i is the radius of the ith ion in meters. For the TA-doped VE resin system, equation (1) can be written as

$$R_j(t) = \frac{6\pi\eta(t)L}{A\left[\frac{C_1 Q_1^2}{r_1} + \frac{C_2 Q_2^2}{r_2} + \frac{C_u Q_u^2}{r_u}\right]}, \tag{2}$$

where the summation term of u represents those contributions to ionic conductivity due to impurity ions already present in the resin system and the subscripts 1 and 2 represent the tetrabutylammonium and acetate ions, respectively.

Impurity ions are inherent to each of the VE resin, initiator, and catalyst components of the resin system. However, because this study dopes the VE resin to a much higher level of conductivity, the contribution of impurity ions to conductance is considered negligible. Equation (2) is only valid for low degrees of conversion. During and after gelation, ionic conductivity is no longer based strictly on the change in viscosity of the resin, but on a more complex change in ionic mobility.

The resistance determined in equation (2) can then be converted into a measured voltage by the following equation:

$$V(t) = 12\left(\frac{R_s}{R_s + R_t(t)}\right), \tag{3}$$

where R_s is a fixed-drop resistance in the DC conductivity monitoring system, which, for this investigation, was equal to 10 MΩ. The voltage profile generated by equation (3) is often easier to interpret than a resistance profile and is frequently used in the manufacturing environment when DC sensing is employed. In the following section, the experimental methodology used to verify and characterize the model inputs, L, A, C_i, and η, and validate the model output, R, is discussed.

3. Experimental Procedures

This section is broken into two major parts: (1) description of the basic components and operation of a SMARTweave DC-sensing system and (2) methodology for the characterization and validation of model inputs and output. The second section is further broken into three parts:

(1) characterization of L and A, (2) characterization of η and C_i and (3) the validation of the model output $R_j(t)$.

3.1 SMARTweave System Components and Operation. SMARTweave is a patented [1] sensor system that measures and tracks the DC conductance of a resin as it flows into an RTM mold and cures. This is done through a noncontacting grid of wires—one set serving as excitation leads and an orthogonal set in a parallel plane serving as sensing leads. The resin acts as a resistor, and, under an applied voltage, current is induced in a circuit containing a drop resistor, called a sense resistor (R_s).

The SMARTweave system used in this study consists of a National Instruments SCXI interface chassis (where the excitation and sense leads are connected), a National Instruments multiplexer (for switching from one set of leads to another), and a computer (for data display and storage). A 12-V power supply provides a DC voltage to the excitation leads. Only one excitation lead is active at any time. The multiplexer sends out a voltage to the excitation leads, and the SCXI chassis monitors the sense leads for an induced current. The induced current is detected as a voltage across R_s.

Figure 3 shows a circuit diagram for a single-node voltage experiment. During a single-node test, excitation voltage remains constant across a single excitation lead. In the presence of a conductive medium, a current is induced in the sense lead and a voltage is created across R_s. Changes in resin resistance, $R_j(t)$, are then recorded as changes in $V_m(t)$ by the SMARTweave software via equation (3). For the single-node experiments performed in this study, a 12-V applied voltage and a 10-MΩ drop resistance were used.

Figure 4 shows a schematic of an SNTC. The SNTC consisted of a clear plastic syringe, which could be varied in size and diameter, and one SMARTweave sense and excitation lead. Sense and excitation leads were made of sewing needles. The plastic syringes were easy to pierce with the sharp sewing needles and formed a tight seal around the needles, preventing any leakage of resin from the cell. Further, the level markings on the syringes assisted in the

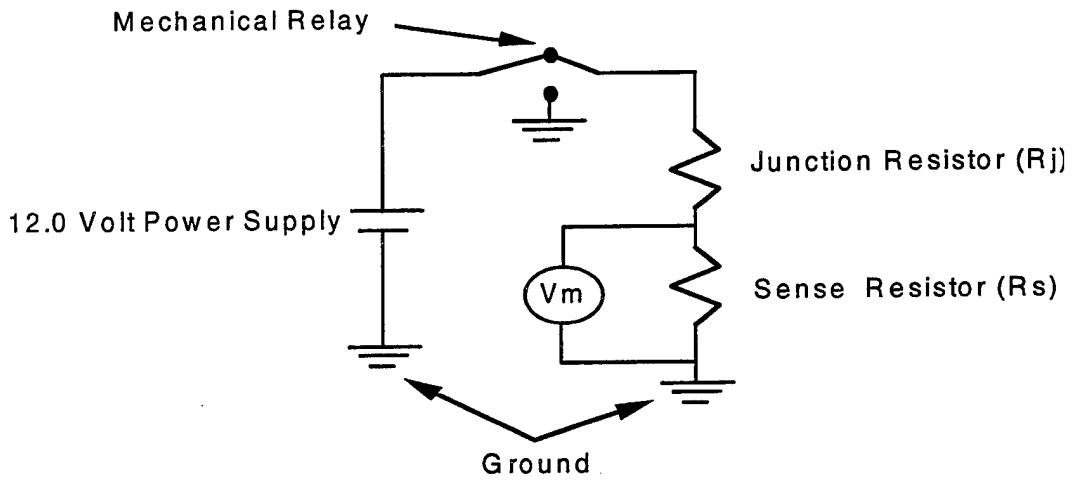

Figure 3. SMARTweave Single-Node Circuit Schematic.

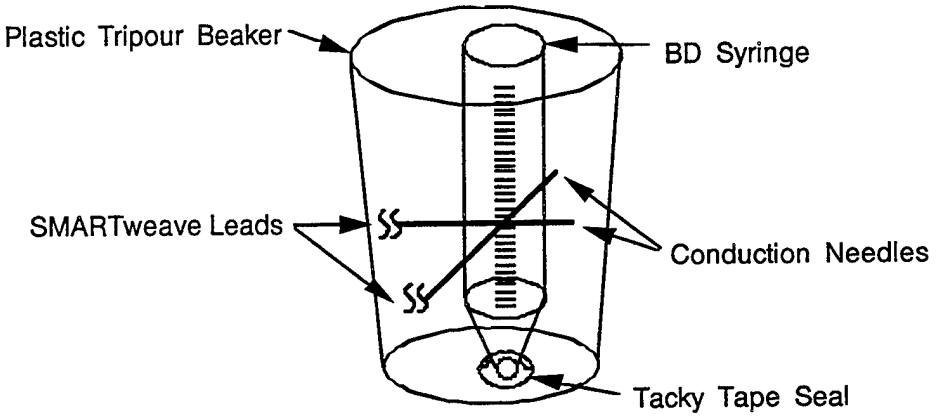

Figure 4. SNTC-1 Configuration.

repeatable placement of needles for separation distance control. Lastly, the surface area of the needles was easy to measure and avoided conductor end effects.

3.2 Model Input Characterization. The geometric model inputs L and A were characterized by measuring (1) changes in R_j with changes in lead separation distance (L), and (2) changes in R_j with changes in conductor surface area (A). A theoretical model of an SNTC electric field was also developed to determine a quantitative estimate of both L and A [6]. The material model inputs were characterized by measuring (1) changes in R_j with changes in ionic

concentration (C_i), (2) changes in R_j with changes in viscosity ($\eta(t)$) as a function of temperature for both a noncuring and curing system, and (3) the effect of curing temperature on SMARTweave voltage [i.e., the validation of $R_j(t)$]. The following sections describe the experimental procedures for the measurements previously listed. Resistance and voltage measurements were collected by the use of a SMARTweave system and an SNTC apparatus.

3.2.1 Characterization of L and A. The effects of lead separation distance and conductor surface area on the resistance of doped VE resin were measured using a SMARTweave system and a series of SNTCs. The series of SNTCs varied in diameter from 8.6 to 21.5 mm. As the diameter of the SNTC was increased, more conductor surface area was exposed. In this way, the effects of increased effective electric field area on resistance could be studied. For each SNTC, the lead separation distance was varied from approximately 7 to 60 mm.

3.2.2 Characterization of C_i and $\eta(t)$. American Society for Testing of Materials (ASTM) standard D257-78 offers a variety of methods for determining the DC conductivity of a material. Figure 5 shows the basic components and dimensions of the DC conductivity cell used in this study. In the DC cell shown in Figure 5, the gap between the inner and out cylinders is filled with the resin and resistance measured with an ohm-meter. For this study, VE resin was doped with an organic salt, with weight-percent concentrations ranging from 0.05 to 7.8 wt-%. A methodology of limiting ionic conductance was then used to determine the concentration of ions as a function of the mass of dopant added [6]. In order to characterize viscosity, the resistance and viscosity of both a noncuring and curing doped VE resin as a function of temperature were measured using a modified SNTC apparatus. The viscosity of doped VE resin was measured using a Brookfield viscometer and small sample adapter (SSA), which was capable of regulating temperature via a water jacket and a circulating water bath. The modified SNTC consisted of two needles whose tips were held 1.0 mm apart by a Teflon ring. The needle tips were then attached to the rim of the SSA and inserted into the resin. Resistance and viscosity were then measured at temperatures ranging from 30 to 70°C for a noncuring system and 30 to 60°C for a curing system.

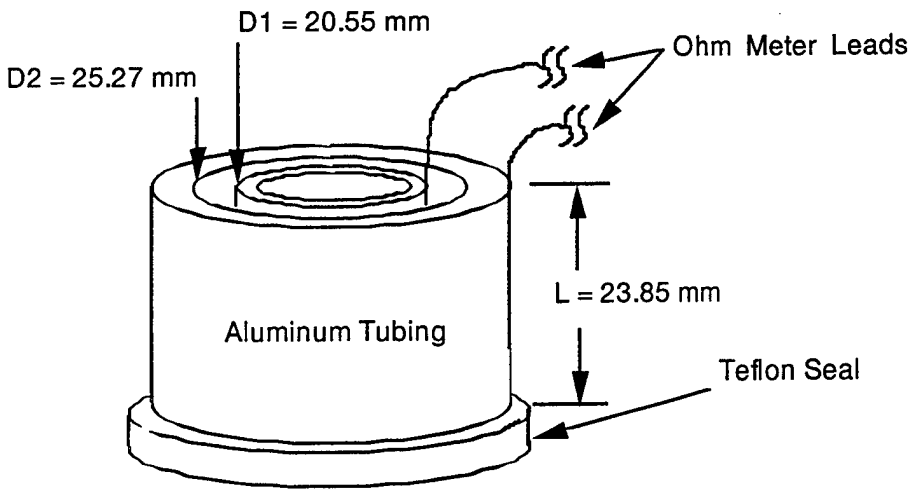

Figure 5. DC Cell Configuration.

3.2.3 Validation of $R_j(t)$. The model output of resistance as a function of time for a curing doped VE resin was studied by isothermal curing of the resin in an SNTC apparatus. Isothermal cure experiments were performed at 30, 40, and 50°C. The samples tested consisted of VE resin with 0.2 wt-% CoNap, 2.0 wt-% Trigonox 239A, and 0.1 wt-% dopant. After the samples were prepared, they were added to the SNTC apparatus and the SMARTweave voltage was monitored. In this way, the changes in resistance are to be coupled with changes in viscosity at varying temperatures. The temperature was monitored to ensure that exotherms during cure were negligible and the isothermal condition was maintained.

The next section provides results of the characterization and validation of the model inputs and output. Emphasis is put on understanding the results of the SNTC experiments in terms of the ionic conductivity of a polymer liquid [i.e., within the range of equation (2)].

4. Results and Discussion

This section is broken into four parts: (1) characterization of L and A, (2) characterization of C_i and $\eta(t)$, (3) validation of model output, and (4) application of the model to the in-situ sensing of viscosity and gelation.

4.1 Characterization of L and A. Figure 6 shows the change in resistance with changes in lead separation distance and conductor surface area. There is a linear behavior between separation distance and resistance for each area tested. The increase in available area, shown in Figure 6 as the wetted conduction surface area, increases the area over which the electric field acts.

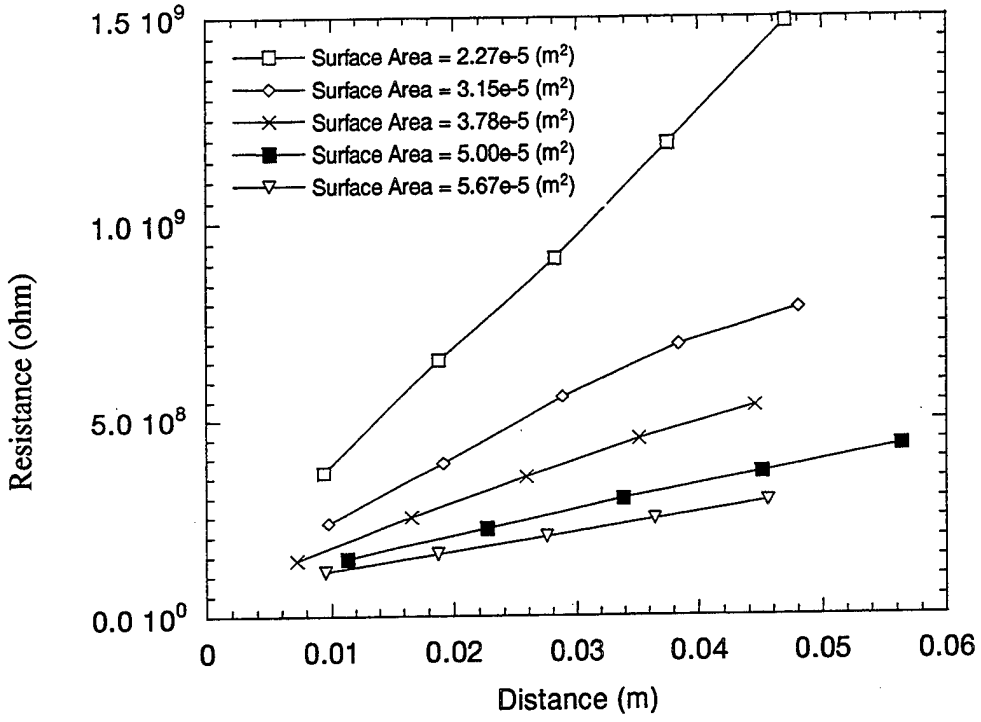

Figure 6. Resistance vs. Distance for Lead Separation and Conductor Surface Area Effect Studies.

As the available area was increased, the slope of resistance vs. separation distance became less. This result is predicted by equation (2). Increases in A will decrease the slope of resistance over separation distance, as shown in equation (4):

$$\frac{R_j(t)}{L} = \frac{6\pi\eta(t)}{A\left[\frac{C_1Q^2}{r_1} + \frac{C_2Q^2}{r_2}\right]} = \frac{\text{const.}}{A}. \qquad (4)$$

The effective area over which the electric field acts within a basic setup of a SMARTweave node was modeled using the following assumptions: (1) steady-state electric field (not changing with time), (2) uniform medium has dielectric constant of unity, (3) conduction surfaces have a uniform charge distribution (λ), and (4) the conductive surfaces are infinite in length. The solution for an infinite wire with a uniform charge distribution is

$$E_r = \frac{2k\lambda}{r}, \tag{5}$$

where k is Boltzman's Constant ($k = 1.3806810^{-23}$ J/K), λ is charge per unit length in coulombs per meter, and r is the radial distance in meters from the axis of the wire [8].

A SMARTweave node can be modeled by superimposing the solutions for two infinite and orthogonal lines of charges, which are separated by a distance d. Figure 7 shows the basic configuration used to model a SMARTweave single-node experiment.

As previously noted, the solution for an infinite line of charge is easily determined. Using the coordinate system shown in Figure 7, the solutions for the electric field strength due to lines 1 and 2 are

$$E_1 = \frac{2k\lambda}{r_1} \tag{6}$$

and

$$E_2 = \frac{2k(-\lambda)}{r_2}. \tag{7}$$

By rewriting r_1 and r_2 in terms of the Cartesian coordinate system used and using the principle of superposition, one gets

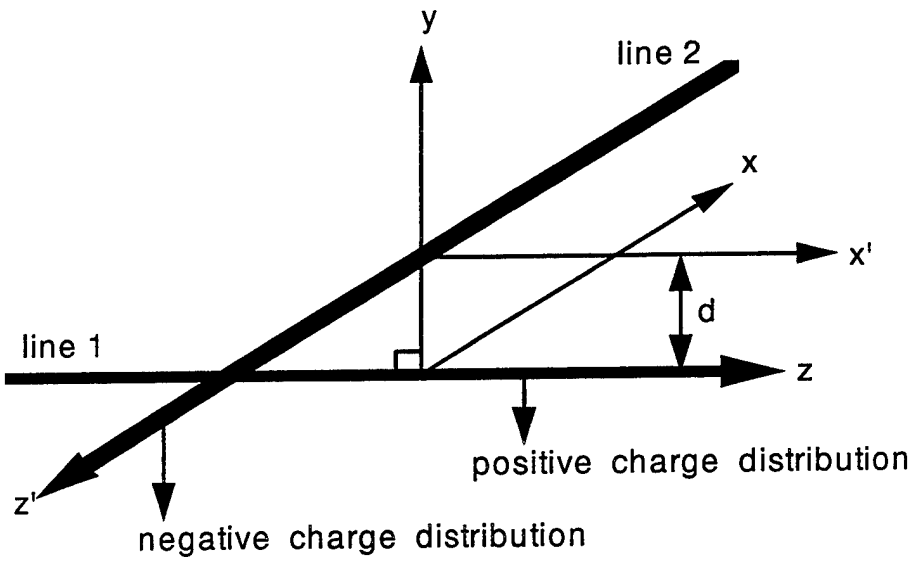

Figure 7. Electric Field Model of a SMARTweave Single Node Experiment.

$$E_1 = \frac{2k\lambda}{\sqrt{x^2 + y^2}} \tag{8}$$

and

$$E_2 = \frac{2k(-\lambda)}{\sqrt{z^2 + (y-d)^2}}. \tag{9}$$

The total electric field strength felt at any point in space is then

$$E_T = E_1 + E_2 = \frac{2k\lambda}{\sqrt{x^2 + y^2}} - \frac{2k\lambda}{\sqrt{z^2 + (y-d)^2}}. \tag{10}$$

Figure 8 shows a contour plot of E_T at d/2 on the y-axis. The total electric field, E_T, is strongest near the intersection, and along the axis, of the lines of charge. Ions located in these regions will feel the strongest pull toward the line of opposite charge, in the direction of increasing voltage potential. Figure 8 shows that an SNTC setup can be treated mainly as a single

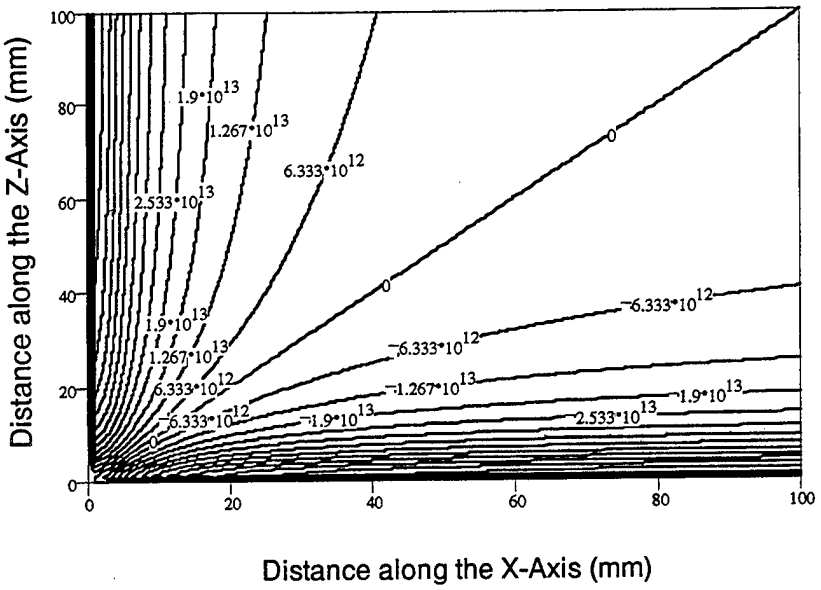

Figure 8. E_T vs. Distance at the Bisector of Two Infinite Lines of Charge. One Line of Charge Lies Along the x-Axis and the Other Along the y-Axis. Contour Values Represent E_T Magnitudes.

line of charge, especially at those regions furthest from the point of intersection. Therefore, an estimation of the average path length that the ions follow can be inferred from equation (5). Equation (5) states that, for the single-line case, the strength of the electric field decays as 1/r. Consequently, the driving forces diminish, and the path length increases such that the number of ions that travel to the lead in any given time period decreases at a rate of 1/r.

The total number of path lengths is equal to the total number of ions present in the system. Further, let the available path lengths vary from 1 Å to 10 mm. Knowing this, the average path length, L, of a 1/r distribution of ions is approximately 0.3 mm. The average path length is independent of concentration; hence, it is valid for any concentration of distribution 1/r. The "effective" area of the electric field created around an infinite wire with a maximum path length of 5 mm is

$$A = 2\pi r^2 = 1.5707 \times 10^{-4}, \tag{11}$$

where A is in square meters.

4.2 Characterization of C_i and $\eta(t)$. Figure 9 shows the change of resistance with changes in the inverse concentration of ions. The concentration of ions was determined from DC conductivity cell measurements and the method of limiting ionic conductivity [6]. The concentration of ionic species was found to be approximately 3.62×10^{19} ions/m^3 for a 0.1 wt-% concentration of TA. The linear behavior of resistance with changes in the inverse concentration of ions shown in Figure 9 confirms the dependence of resistance on the concentration of ions as modeled by equation (3), which states

$$R_j(t) = \frac{6\pi\eta(t)L}{A\sum_i \frac{C_i Q_i^2}{r_i}} \propto \frac{\text{const.1}}{\sum_i \text{const.2} \cdot C_i}. \tag{12}$$

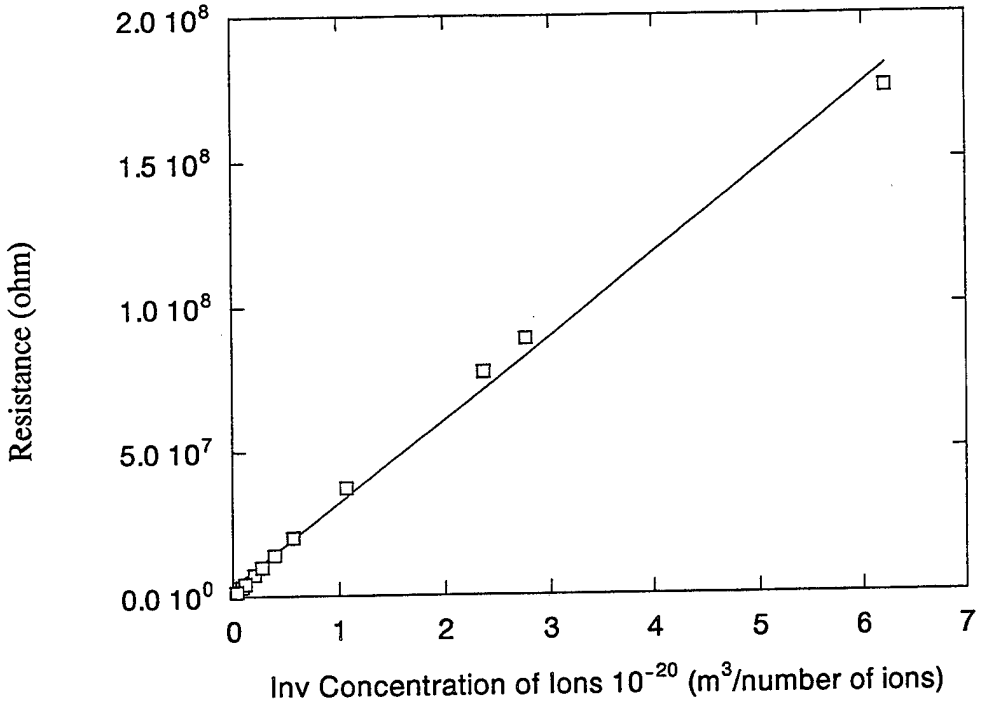

Figure 9. Conductivity vs. Inverse Concentration of Ions. Data Points Are Shown Along With a Linear Curve Fit.

Figure 10 shows the change in resistance with changes in viscosity for a noncuring TA-doped VE resin. The linear relationship between changes in resistance with changes in viscosity seen

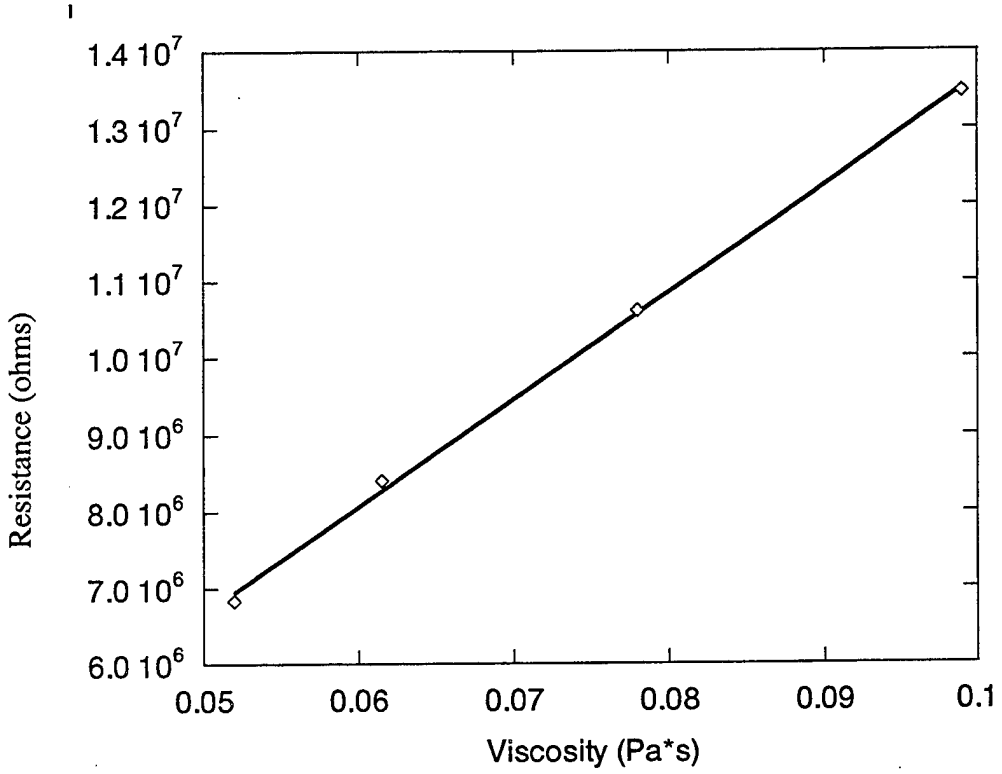

Figure 10. Resistance vs. Viscosity. Linear Fit Shown With Data Points. Data Points Shown Along With a Linear Curve Fit.

in Figure 10 confirms the dependence of resistance on viscosity as modeled by equation (3), which states that

$$R_j(t) = \frac{6\pi\eta(t)L}{A\sum_i \frac{C_i Q_i^2}{r_i}} = \text{const.}\,\eta(t)\,. \tag{13}$$

Figures 6, 9, and 10, along with equations (4), (12), and (13), have proven that the model of polymer electrolytes presented in equation (3) is a valid means of understanding the relationship between resistance and L, A, C_i, and $\eta(t)$. Therefore, it is now useful to understand the relationship between resistance and viscosity of a reacting polymer. This is done by monitoring the viscosity and resistance of a curing VE resin at a different temperature; but, first, it is desirable to understand the change in viscosity of a noncuring VE resin with temperature.

Figure 11 shows the change in viscosity with changes in temperature for a noncuring TA-doped VE resin. The behavior shown in Figure 11 is typical of most polymeric systems [9]. The viscosity vs. temperature behavior of a noncuring TA-doped VE resin follows the following form:

$$\eta(T) = 8.522\times10^{-8} e^{\frac{35,218}{RT}} (Pa-s), \tag{14}$$

where T is temperature in Kelvin, R is the universal gas constant, and the correlation coefficient is 0.99656.

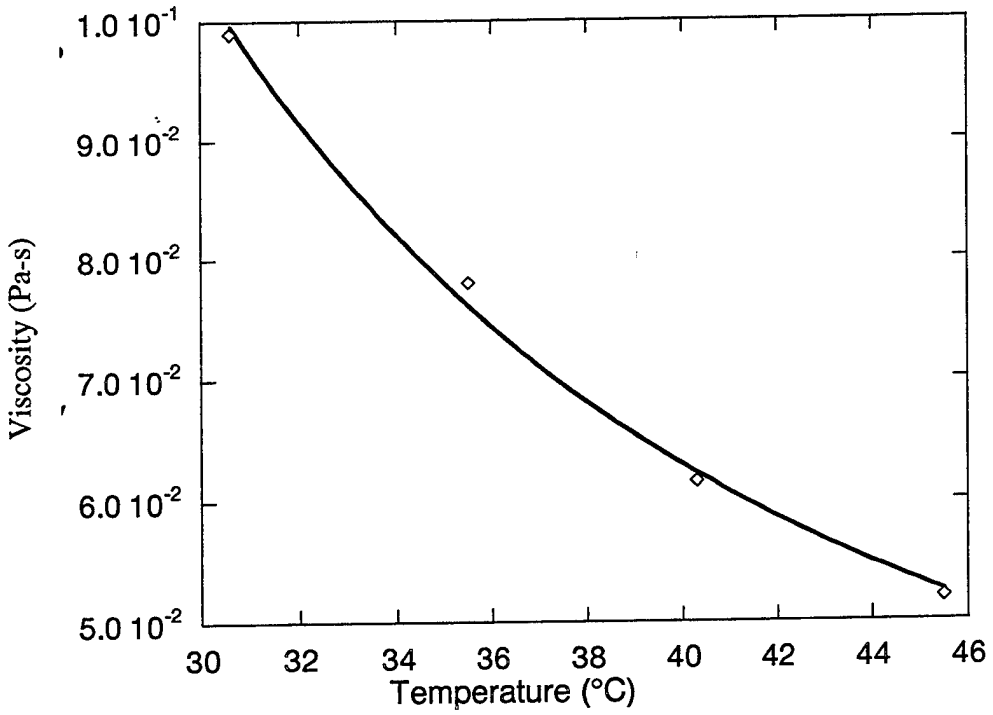

Figure 11. Viscosity vs. Temperature for TA-Doped VE Resin. Data Points Are Shown Along With an Arrhenius Curve Fit.

Now that the estimates for L, A, C_i, and $\eta(T)$ have been determined, a theoretical estimate of resistance can be calculated using equation (2). The theoretical estimate of the resistance of an

SNTC apparatus for a noncuring TA-doped VE in which a 1-V drop across a 0.005-m lead separation distance occurs for a 0.1-wt-% TA-doped VE resin with a viscosity of 0.1 Pa-s at room temperature is 864 MΩ. The experimental value expected for such a case is 110 MΩ. The theoretical estimate is within an order of magnitude of the experimentally determined value. Given the variability in resin chemistry, experimental setup, and data collection, this is a very good estimate of the resistance of an SNTC configuration and doped VE resin system.

The following section validates the model output of $R_j(t)$ for a curing VE resin. First, an understanding of how resistance and viscosity of a reacting polymer change as a function of temperature is developed. Then, equation (2) is applied and analyzed to determine its ability to sense gelation.

4.3 Validation of $R_j(t)$. In order to validate the ionic conductivity of a curing VE resin, it is first necessary to characterize the change in viscosity of a curing resin as a function of cure temperature. Figure 12 shows the viscosity of curing TA-doped VE resin at different cure temperatures. Increases in isothermal cure temperature are followed by a decrease in gelation times. Remember, gelation can be defined as the point at which the resin viscosity tends toward infinity.

The next step in the validation of $R_j(t)$ is the characterization of ionic conductance as a function of cure temperature. Figure 13 shows SMARTweave voltage vs. time for the isothermal cure experiments. The initial regions of the voltage curves show a rise in voltage as the resin samples reach the temperature of the water bath. Once the sample reaches the temperature of the water bath, it remains at that temperature. As cure and network formation start to increase, the voltage signal starts to drop and eventually becomes negligible. Increases in cure temperature result in increases in peak voltage (i.e., conductivity) and decrease periods of measurable voltage. This results from an increased rate of reaction, which increases with increasing temperature.

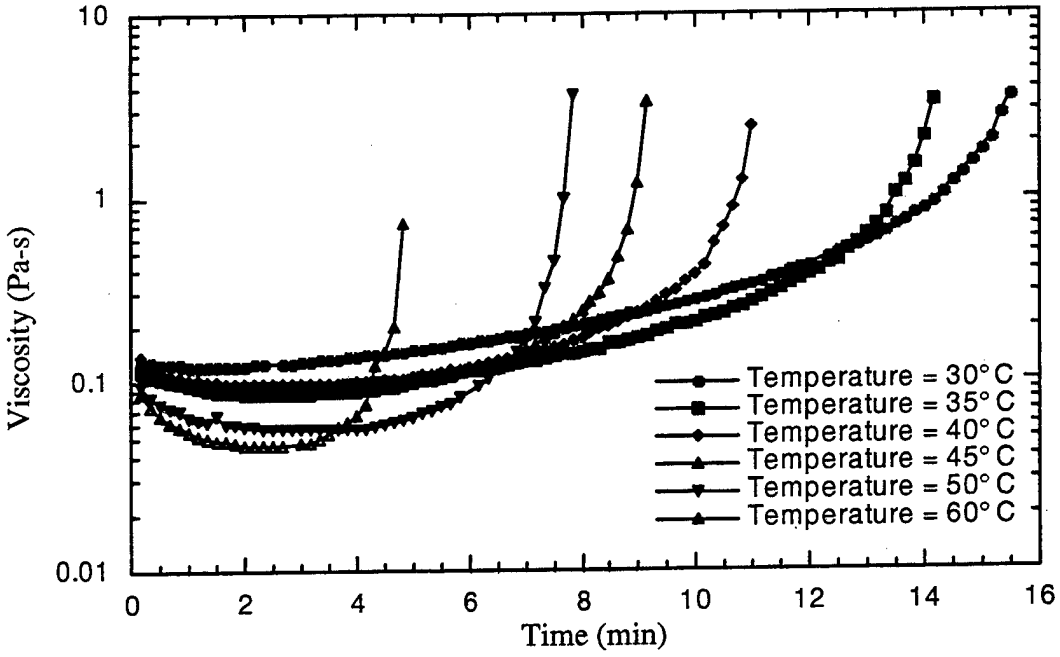

Figure 12. Viscosity vs. Time of Curing TA-Doped VE Resin.

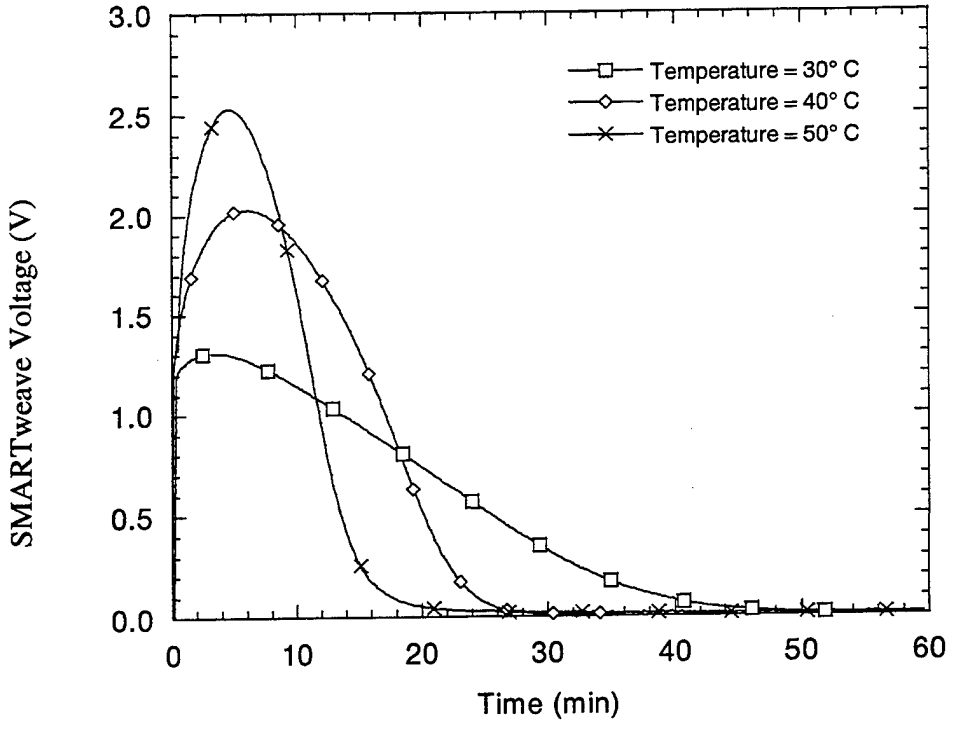

Figure 13. Isothermal Conductance vs. Time. Markers Do Not Represent All Data Points Taken. All Data Points Fall on Lines Connecting Markers.

Another way of viewing the SMARTweave data shown in Figure 13 is to plot the rate of change of the SMARTweave voltage vs. time (dV/dt). Figure 14 shows the rate change of SMARTweave voltage vs. time for isothermal cure temperatures of 30, 40, and 50°C. The minimum experienced in the rate change of voltage (dV/dt_{min}) is a function of cure temperature. As cure temperature increases, dV/dt_{min} becomes more defined and greater in magnitude.

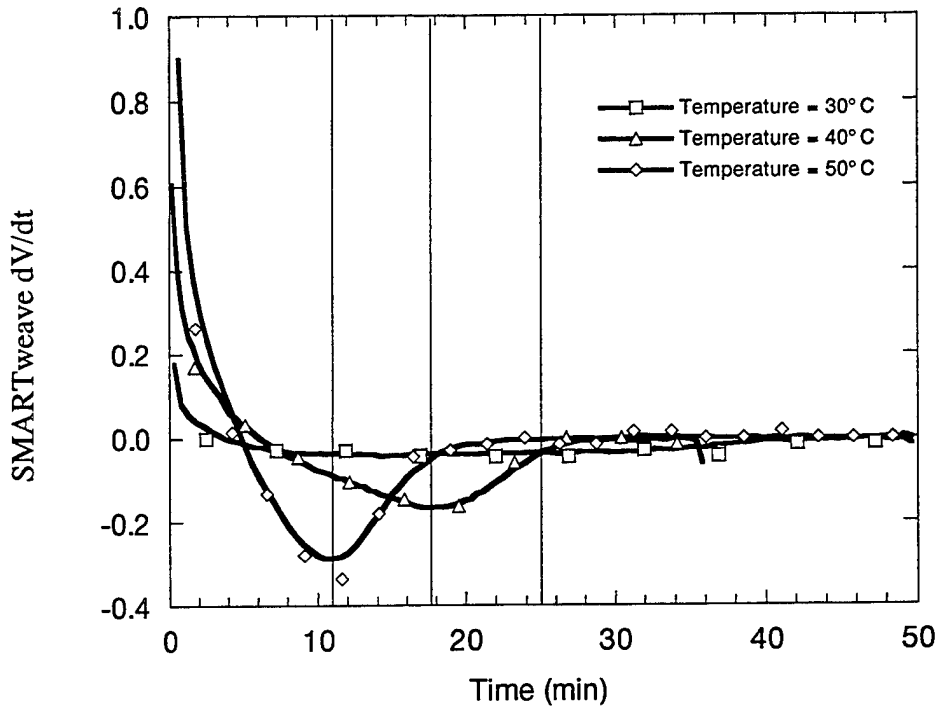

Figure 14. SMARTweave Voltage vs. Time. Markers Do Not Represent All Data Points Taken. All Data Points Fall on Lines Connecting Markers. Vertical Lines Mark the Minimum Points of Each Curve.

Equation (3) can be rearranged and combined with equation (4) to predict the rate change of SMARTweave voltage with time. The rate change of voltage as a function of $\eta(t)$, L, A, C_i, and r_i is

$$\frac{dV}{dt} = -12\frac{R_s + \frac{dR_j(t)}{dt}}{(R_s + R_j(t))^2}. \qquad (15)$$

Assuming that only viscosity changes with time,

$$\frac{dR_j(t)}{dt} = \frac{6\pi + \frac{d\eta(t)}{dt}L}{A\left[\frac{C_1Q_1^2}{r_1} + \frac{C_2Q_2^2}{r_2}\right]}, \tag{16}$$

where

$$R_s = 10\ M\Omega \tag{17}$$

and

$$R_j(t) = \frac{6\pi\eta(t)}{A\left[\frac{C_1Q^2}{r_1} + \frac{C_2Q^2}{r_2}\right]}. \tag{18}$$

Using the viscosity curves shown in Figure 11, the rate change of SMARTweave voltage can now be predicted by inserting the values for $\eta(t)$ and $d\eta(t)/dt$ into equations (15) and (17). Figure 15 shows the predicted dV/dt curves for TA-doped VE resin at 30, 40, and 50°C.

As can be seen from Figure 15, equation (3) also predicts a dV/dt_{min}. The minimum occur at the onset of gelation, at which time the viscosity of the VE resin starts an exponential climb toward infinity. As cure progresses, network formation can cause L to increase as the pathways to ionic mobility decrease in number and become more tortuous in nature. Therefore, once dV/dt_{min} has been reached, equation (8) can no longer be used to predict the electrical properties of a curing TA-doped VE resin.

The application of equation (3) to processing is clear. Once dV/dt_{min} has been detected, the flow of resin within the part becomes severely impeded. In other words, dV/dt_{min} can be used to determine the point at which resin infusion into the preform will no longer be practical. The

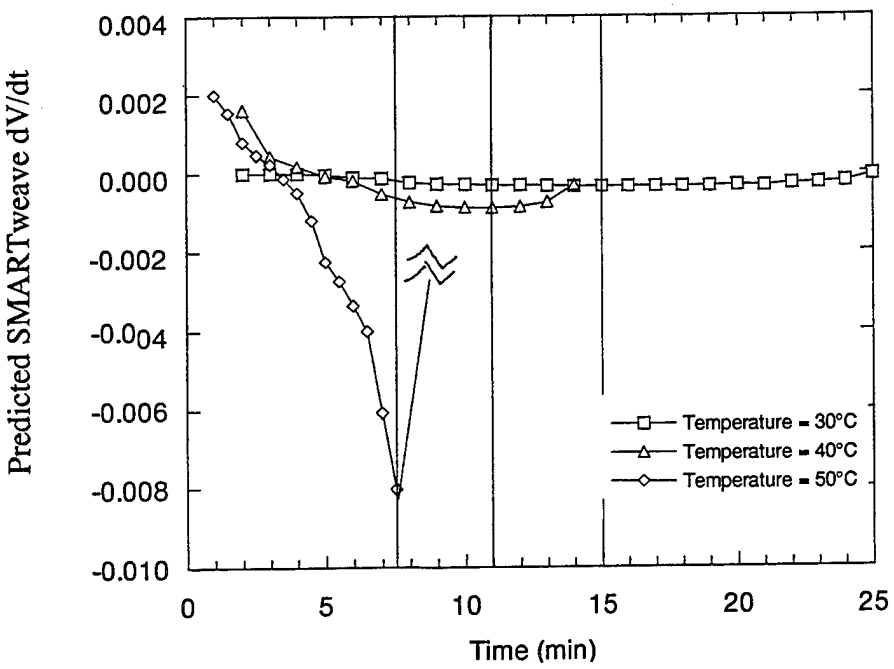

Figure 15. Predicted SMARTweave dV/dt vs. Time. Lines Mark the Predicted dV/dt_{min}.

following section couples the lessons learned in the previous sections with equation (2) to develop a method by which the DC sensing can be used to monitor the viscosity of a curing resin system.

4.4 Application of Model to DC Sensing of Viscosity. There is yet another use of equation (3) and dV/dt_{min}. If all parameters except viscosity in equation (3) are assumed constant, normalization of equation (3) yields

$$\eta(t) = \eta_0(T)\frac{R(t)}{R_0}, \tag{19}$$

where η_0 (T) and R_0 are the viscosity and resistance at time t = 0, respectively. Equation (19) can be used to calculate the viscosity vs. time of a curing resin using the SMARTweave voltage profile. Figure 16 shows the predicted viscosity for isothermal cure SNTC experiments at 30, 40, and 50°C. For SNTC tests at 30, 40, and 50° C, the dV/dt_{min} occurs before the viscosity reaches 0.15 Pa-s.

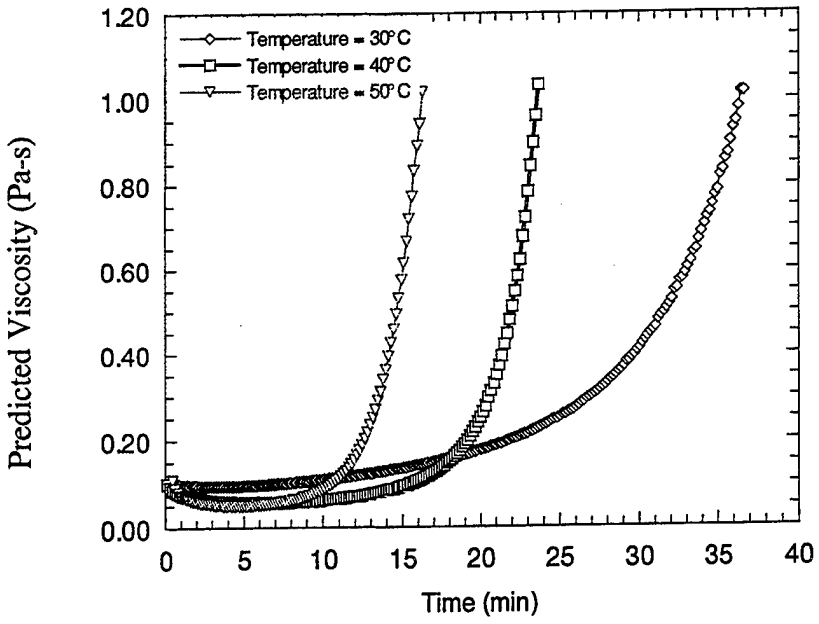

Figure 16. Calculated Viscosity vs. Time for SNTC-4 Isothermal Cure Studies.

Once the viscosity reaches 0.15 Pa-s, it begins to increase rapidly, reflecting the initial formation of a rigid cross-linked network of VE and styrene polymer. After a viscosity of 0.15 Pa-s has been reached, equations (3) and (19) are no longer valid. This is due to the increase in L with network formation.

5. Conclusion

In this investigation, a model of the resistance of a TA-doped VE resin, up to gelation, was developed and the material and geometric parameters of that model were successfully characterized. A single SMARTweave sensor-node configuration was modeled to yield estimates of resistance, viscosity, and onset of gelation for a curing resin system. SMARTweave was shown to be an effective system for in-situ monitoring of the viscosity of a curing VE resin and as a viable tool for determining the onset of gelation. It was determined that the onset of gelation causes a minimum in the rate of change of ionic conductivity and that the viscosity of a curing TA-doped VE resin system can be determined through measurements of ionic conductivity.

6. References

1. Walsh, S. M. "In-Situ Sensor Method and Device." U.S. Patent No. 5,210,499, 11 May 1993.

2. Don, R. C., K. Bernetich, J. W. Gillespie, Jr., and M. Louderback. CCM Technical Report No. 97-12, University of Delaware, Newark, DE, 1997.

3. Fink, B. K., S. M. Walsh, D. C. DeSchepper, J. W. Gillespie, Jr., R. L. McCullough, R. C. Don, and B. J. Waibel. "Advances in Resin Transfer Molding Flow Monitoring Using SMARTweave Sensors." *Proceedings of the ASME Materials Division*, vol. 69.2, pp. 999–1015, International Mechanical Engineering Conference and Exposition, 1995.

4. Fink, B. K., S. M. Walsh, D. C. DeSchepper, J. Kleinmeyer, S. Bickerton, and R. C. Don. "Development of a Two-Sided Wiring Scheme for Resin Transfer Molding Flow Monitoring Using SMARTweave Sensor." CCM Technical Report No. 95-08, University of Delaware, Newark, DE, 1995.

5. Walsh, S. M., and B. K. Fink. "Streamlining Material Aquistion Using Intelligent Processing and Prototyping." *Proceedings of 20th Army Science Conference*, Norfolk, VA, 1996.

6. England, K. M. "Direct Current Sensing of Viscosity and Degree of Cure of Vinyl-Ester Resins." Masters Thesis, University of Delaware, Summer, 1997.

7. Schwab, S. D., R. L. Levy, and G. G. Glover. "Sensor System for Monitoring Impregnation and Cure During Resin Transfer Molding." *Polymer Composites*, vol. 17, no. 2, pp. 312–316, April 1996.

8. Tipler, P. A. *Physics: For Scientists and Engineers.* New York, NY: Worth Publishers, Third Edition, 1991.

9. Rosen, S. L. *Fundamental Principles of Polymeric Materials.* New York, NY: John Wiley and Sons, Inc., 1993.

INTENTIONALLY LEFT BLANK.

NO. OF COPIES ORGANIZATION

2 DEFENSE TECHNICAL INFORMATION CENTER
DTIC DDA
8725 JOHN J KINGMAN RD
STE 0944
FT BELVOIR VA 22060-6218

1 HQDA
DAMO FDQ
D SCHMIDT
400 ARMY PENTAGON
WASHINGTON DC 20310-0460

1 OSD
OUSD(A&T)/ODDDR&E(R)
R J TREW
THE PENTAGON
WASHINGTON DC 20301-7100

1 DPTY CG FOR RDA
US ARMY MATERIEL CMD
AMCRDA
5001 EISENHOWER AVE
ALEXANDRIA VA 22333-0001

1 INST FOR ADVNCD TCHNLGY
THE UNIV OF TEXAS AT AUSTIN
PO BOX 202797
AUSTIN TX 78720-2797

1 DARPA
B KASPAR
3701 N FAIRFAX DR
ARLINGTON VA 22203-1714

1 NAVAL SURFACE WARFARE CTR
CODE B07 J PENNELLA
17320 DAHLGREN RD
BLDG 1470 RM 1101
DAHLGREN VA 22448-5100

1 US MILITARY ACADEMY
MATH SCI CTR OF EXCELLENCE
DEPT OF MATHEMATICAL SCI
MADN MATH
THAYER HALL
WEST POINT NY 10996-1786

NO. OF COPIES ORGANIZATION

1 DIRECTOR
US ARMY RESEARCH LAB
AMSRL DD
2800 POWDER MILL RD
ADELPHI MD 20783-1197

1 DIRECTOR
US ARMY RESEARCH LAB
AMSRL CS AS (RECORDS MGMT)
2800 POWDER MILL RD
ADELPHI MD 20783-1145

3 DIRECTOR
US ARMY RESEARCH LAB
AMSRL CI LL
2800 POWDER MILL RD
ADELPHI MD 20783-1145

ABERDEEN PROVING GROUND

4 DIR USARL
AMSRL CI LP (BLDG 305)

NO. OF COPIES	ORGANIZATION
1	DIRECTOR USARL AMSRL CP CA D SNIDER 2800 POWDER MILL RD ADELPHI MD 20783
1	COMMANDER USA ARDEC AMSTA AR FSE T GORA PICATINNY ARSENAL NJ 07806-5000
3	COMMANDER USA ARDEC AMSTA AR TD PICATINY ARSENAL NJ 078806-5000
5	COMMANDER USA TACOM AMSTA JSK S GOODMAN J FLORENCE AMSTA TR D B RAJU L HINOJOSA D OSTBERG WARREN MI 48397-5000
5	PM SADARM SFAE GCSS SD COL B ELLIS M DEVINE W DEMASSI J PRITCHARD S HROWNAK PICATINNY ARSENAL NJ 07806-5000
1	COMMANDER USA ARDEC F MCLAUGHLIN PICATINNY ARSENAL NJ 07806-5000

NO OF. COPIES	ORGANIZATION
5	COMMANDER USA ARDEC AMSTA AR CCH S MUSALLI R CARR M LUCIANO T LOUCEIRO PICATINNY ARSENAL NJ 07806-5000
4	COMMANDER USA ARDEC AMSTA AR (2CPS) E FENNEL (2 CPS) PICATINNY ARSENAL NJ 07806-5000
1	COMMANDER USA ARDEC AMSTA AR CCH P J LUTZ PICATINNY ARSENAL NJ 07806-5000
1	COMMANDER USA ARDEC AMSTA AR FSF T C LIVECCHIA PICATINNY ARSENAL NJ 07806-5000
1	COMMANDER USA ARDEC AMSTA AR QAC T/C C PATEL PICATINNY ARSENAL NJ 07806-5000
2	COMMANDER USA ARDEC AMSTA AR M D DEMELLA F DIORIO PICATINNY ARSENAL NJ 07806-5000

NO. OF COPIES	ORGANIZATION
3	COMMANDER USA ARDEC AMSTA AR FSA A WARNASH B MACHAK M CHIEFA PICATINNY ARSENAL NJ 07806-5000
1	COMMANDER SMCWV QAE Q B VANINA BLDG 44 WATERVLIET ARSENAL WATERVLIET NY 12189-4050
1	COMMANDER SMCWV SPM T MCCLOSKEY BLDG 253 WATERVLIET ARSENAL WATERVLIET NY 12189-4050
8	DIRECTORECTOR BENET LABORATORIES AMSTA AR CCB J KEANE J BATTAGLIA J VASILAKIS G FFIAR V MONTVORI G DANDREA R HASENBEIN AMSTA AR CCB R S SOPOK WATERVLIET NY 12189-4050
1	COMMANDER SMCWV QA QS K INSCO WATERVLIET NY 12189-4050
1	COMMANDER PRODUCTION BASE MODERN ACTY USA ARDEC AMSMC PBM K PICATINNY ARSENAL NJ 07806-5000

NO OF. COPIES	ORGANIZATION
1	COMMANDER USA BELVOIR RD&E CTR STRBE JBC FT BELVOIR VA 22060-5606
2	COMMANDER USA ARDEC AMSTA AR FSB G M SCHIKSNIS D CARLUCCI PICATINNY ARSENAL NJ 07806-5000
1	US ARMY COLD REGIONS RESEARCH & ENGINEERING CTR P DUTTA 72 LYME RD HANVOVER NH 03755
1	DIRECTOR USARL AMSRL WT L D WOODBURY 2800 POWDER MILL RD ADELPHI MD 20783-1145
1	COMMANDER USA MICOM AMSMI RD W MCCORKLE REDSTONE ARSENAL AL 35898-5247
1	COMMANDER USA MICOM AMSMI RD ST P DOYLE REDSTONE ARSENAL AL 35898-5247
1	COMMANDER USA MICOM AMSMI RD ST CN T VANDIVER REDSTONE ARSENAL AL 35898-5247
3	US ARMY RESEARCH OFFICE A CROWSON K LOGAN J CHANDRA PO BOX 12211 RESEARCH TRIANGLE PARK NC 27709-2211

NO. OF COPIES	ORGANIZATION
3	US ARMY RESEARCH OFFICE ENGINEERING SCIENCES DIV R SINGLETON G ANDERSON K IYER PO BOX 12211 RESEARCH TRIANGLE PARK NC 27709-2211
5	PM TMAS SFAE GSSC TMA COL PAWLICKI K KIMKER E KOPACZ R ROESER B DORCY PICATINNY ARSENAL NJ 07806-5000
1	PM TMAS SFAE GSSC TMA SMD R KOWALSKI PICATINNY ARSENAL NJ 07806-5000
3	PEO FIELD ARTILLERY SYSTEMS SFAE FAS PM H GOLDMAN T MCWILLIAMS T LINDSAY PICATINNY ARSENAL NJ 07806-5000
2	PM CRUSADER G DELCOCO J SHIELDS PICATINNY ARSENAL NJ 07806-5000
3	NASA LANGLEY RESEARCH CTR MS 266 AMSRL VS W ELBER F BARTLETT JR C DAVILA HAMPTON VA 23681-0001

NO OF. COPIES	ORGANIZATION
2	COMMANDER DARPA S WAX 2701 N FAIRFAX DR ARLINGTON VA 22203-1714
6	COMMANDER WRIGHT PATTERSON AFB WL FIV A MAYER WL MLBM S DONALDSON T BENSON-TOLLE C BROWNING J MCCOY F ABRAMS 2941 P ST STE 1 DAYTON OH 45433
2	NAVAL SURFACE WARFARE CTR DAHLGREN DIV CODE G06 R HUBBARD CODE G 33 C DAHLGREN VA 22448
1	NAVAL RESEARCH LAB I WOLOCK CODE 6383 WASHINGTON DC 20375-5000
1	OFFICE OF NAVAL RESEARCH MECH DIV Y RAJAPAKSE CODE 1132SM ARLINGTON VA 22271
1	NAVAL SURFACE WARFARE CTR CRANE DIV M JOHNSON CODE 20H4 LOUISVILLE KY 40214-5245
1	DAVID TAYLOR RESEARCH CTR SHIP STRUCTURES & PROTECTION DEPT J CORRADO CODE 1702 BETHESDA MD 20084
2	DAVID TAYLOR RESEARCH CTR R ROCKWELL W PHYILLAIER BETHESDA MD 20054-5000

NO. OF COPIES	ORGANIZATION
1	DEFENSE NUCLEAR AGENCY INNOVATIVE CONCEPTS DIV R ROHR 6801 TELEGRAPH RD ALEXANDRIA VA 22310-3398
1	EXPEDITIONARY WARFARE DIV N85 F SHOUP 2000 NAVY PENTAGON WASHINGTON DC 20350-2000
1	OFFICE OF NAVAL RESEARCH D SIEGEL 351 800 N QUINCY ST ARLINGTON VA 22217-5660
7	NAVAL SURFACE WARFARE CTR J H FRANCIS CODE G30 D WILSON CODE G32 R D COOPER CODE G32 E ROWE CODE G33 T DURAN CODE G33 L DE SIMONE CODE G33 DAHLGREN VA 22448
1	COMMANDER NAVAL SEA SYSTEM CMD P LIESE 2351 JEFFERSON DAVIS HIGHWAY ARLINGTON VA 22242-5160
1	NAVAL SURFACE WARFARE CTR M E LACY CODE B02 17320 DAHLGREN RD DAHLGREN VA 22448
1	NAVAL WARFARE SURFACE CTR TECH LIBRARY CODE 323 17320 DAHLGREN RD DAHLGREN VA 22448
4	DIR LLNL R CHRISTENSEN S DETERESA F MAGMESS M FINGER PO BOX 808 LIVERMORE CA 94550

NO OF. COPIES	ORGANIZATION
2	DIRECTOR LLNL F ADDESSIO MS B216 J REPPA MS F668 PO BOX 1633 LOS ALAMOS NM 87545
3	UNITED DEFENSE LP 4800 EAST RIVER DR P JANKE MS170 T GIOVANETTI MS236 B VAN WYK MS 389 MINNEAPOLIS MN 55421-1498
4	DIRECTOR SANDIA NATIONAL LAB APPLIED MECHANICS DEPT DIV 8241 W KAWAHARA K PERANO D DAWSON P NIELAN PO BOX 969 LIVERMORE CA 94550-0096
1	BATTALLE C R HARGREAVES 505 KNIG AVE COLUMBUS OH 43201-2681
1	PACIFIC NORTHWEST LAB M SMITH PO BOX 999 RICHLAND WA 99352
1	LLNL M MURPHY PO BOX 808 L 282 LIVERMORE CA 94550
10	UNIV OF DELAWARE CTR FOR OCMPOSITE MATERIALS J GILLESPIE 201 SPENCER LAB NEWARK DE 19716

NO. OF COPIES	ORGANIZATION
2	THE U OF TEXAS AT AUSTIN CTR ELECTROMECHANICS A WALLIS J KITZMILLER 10100 BURNET RD AUSTIN TX 78758-4497
1	AAI CORPORATION T G STASTNY PO BOX 126 HUNT VALLEY MD 21030-0126
1	SAIC D DAKIN 2200 POWELL ST STE 1090 EMERYVILLE CA 94608
1	SAIC M PALMER 2109 AIR PARK RD S E ALBUQUERQUE NM 87106
1	SAIC R ACEBAL 1225 JOHNSON FERRY RD STE 100 MARIETTA GA 30068
1	SAIC G CHRYSSOMALLIS 3800 W 80TH ST STE 1090 BLOOMINGTON MN 55431
6	ALLIANT TECHSYSTEMS INC C CANDLAND R BECKER L LEE R LONG D KAMDAR G KASSUELKE 600 2ND ST NE HOPKINS MN 55343-8367
1	CUSTOM ANALYTICAL ENGR SYS INC A ALEXANDER 13000 TENSOR LANE NE FLINTSTONE MD 21530

NO OF. COPIES	ORGANIZATION
1	NOESIS INC 1110 N GLEBE RD STE 250 ARLINGTON VA 22201-4795
1	ARROW TECH ASSO 1233 SHELBURNE RD STE D 8 SOUTH BURLINGTON VT 05403-7700
5	GEN CORP AEROJET D PILLASCH T COULTER C FLYNN D RUBAREZUL M GREINER 1100 WEST HOLLYVALE ST AZUSA CA 91702-0296
1	NIST STRUCTURE & MECHANICS GRP POLYMER DIV POLYMERS RM A209 G MCKENNA GAITHERSBURG MD 20899
1	GENERAL DYNAMICS LAND SYSTEM DIVISION D BARTLE PO BOX 1901 WARREN MI 48090
4	INSTITUTE FOR ADVANCED TECHNOLOGY H FAIR P SULILVAN W REINECKE I MCNAB 4030 2 W BRAKER LN AUSTIN TX 78759
1	PM ADVANCED CONCEPTS LORAL VOUGHT SYSTEMS J TAYLOR MS WT 21 PO BOX 650003 DALLAS TX 76265-0003

NO. OF COPIES	ORGANIZATION
2	UNITED DEFENSE LP P PARA G THOMASA 1107 COLEMAN AVE BOX 367 SAN JOSE CA 95103
1	MARINE CORPS SYSTEMS CMD PM GROUND WPNS COL R OWEN 2083 BARNETT AVE STE 315 QUANTICO VA 22134-5000
1	OFFICE OF NAVAL RES J KELLY 800 NORTH QUINCEY ST ARLINGTON VA 22217-5000
1	NAVSEE OJRI G CAMPONESCHI 2351 JEFFERSON DAVIS HWY ARLINGTON VA 22242-5160
1	USAF WL MLS O L A HAKIM 5525 BAILEY LOOP 243E MCCLELLAN AFB CA 55552
1	NASA LANGLEY J MASTERS MS 389 HAMPTON VA 23662-5225
2	FAA TECH CTR D OPLINGER AAR 431 P SHYPRYKEVICH AAR 431 ATLANTIC CITY NJ 08405
1	NASA LANGLEY RC CC POE MS 188E NEWPORT NEWS VA 23608
1	USAF WL MLBC E SHINN 2941 PST STE 1 WRIGHT PATTERSON AFB OH 45433-7750

NO OF. COPIES	ORGANIZATION
4	NIST POLYMERS DIVISION R PARNAS J DUNKERS M VANLANDINGHAM D HUNSTON GAITHERSBURG MD 20899
1	OAK RIDGE NATIONAL LAB A WERESZCZAK BLDG 4515 MS 6069 PO BOX 2008 OAKRIDGE TN 37831-6064
1	COMMANDER USA ARDEC INDUSTRIAL ECOLOGY CTR T SACHAR BLDG 172 PICATINNY ARSENAL NJ 07806-5000
1	COMMANDER USA ATCOM AVIATION APPLIED TECH DIR J SCHUCK FT EUSTIS VA 23604
1	COMMANDER USA ARDEC AMSTA AR SRE D YEE PICATINNY ARSENAL NJ 07806-5000
1	COMMANDER USA ARDEC AMSTA AR QAC T D RIGOGLIOSO BLDG 354 M829E3 IPT PICATINNY ARSENAL NJ 07806-5000

NO. OF COPIES ORGANIZATION

7 COMMANDER
USA ARDEC
AMSTA AR CCH B
B KONRAD
E RIVERA
G EUSTICE
S PATEL
G WAGNECZ
R SAYER
F CHANG
BLDG 65
PICATINNY ARSENAL NJ
07806-5000

6 DIRECTOR
US ARMY RESEARCH LAB
AMSRL WM MB
A ABRAHAMIAN
M BERMAN
A FRYDMAN
T LI
W MCINTOSH
E SZYMANSKI
2800 POWDER MILL RD
ADELPHI MD 20783-1197

ABERDEEN PROVING GROUND

66 DIR USARL
AMSRL CI
AMSRL CI C
W STUREK
AMSRL CI CB
R KASTE
AMSRL CI S
A MARK
AMSRL SL B
AMSRL SL BA
AMSRL SL BE
D BELY
AMSRL WM B
A HORST
E SCHMIDT
AMSRL WM BE
G WREN
C LEVERITT
D KOOKER

NO OF. COPIES ORGANIZATION

AMSRL WM BC
P PLOSTINS
D LYON
J NEWILL
AMSRL WM BD
S WILKERSON
R FIFER
B FORCH
R PESCE RODRIGUEZ
B RICE
AMSRL WM
D VIECHNICKI
G HAGNAUER
J MCCAULEY
AMSRL WM MA
R SHUFORD
S MCKNIGHT
L GHIORSE
AMSRL WM MB
V HARIK
J SANDS
W DRYSDALE
J BENDER
T BLANAS
T BOGETTI
R BOSSOLI
L BURTON
S CORNELISON
P DEHMER
R DOOLEY
B FINK
G GAZONAS
S GHIORSE
D GRANVILLE
D HOPKINS
C HOPPEL
D HENRY
R KASTE
M LEADORE
R LIEB
E RIGAS
D SPAGNUOLO
W SPURGEON
J TZENG
AMSRL WM MC
J BEATTY
AMSRL WM MD
W ROY
AMSRL WM T
B BURNS

NO. OF COPIES	ORGANIZATION
	ABERDEEN PROVING GROUND (CONT)
	AMSRL WM TA
	W GILLICH
	E RAPACKI
	T HAVEL
	AMSRL WM TC
	R COATES
	W DE ROSSET
	AMSRL WM TD
	W BRUCHEY
	A D GUPTA
	AMSRL WM BA
	F BRANDON
	W D AMICO
	AMSRL WM BR
	J BORNSTEIN
	AMSRL WM TE
	A NIILER
	AMSRL WM BF
	J LACETERA

NO OF. COPIES	ORGANIZATION

INTENTIONALLY LEFT BLANK.

REPORT DOCUMENTATION PAGE

Form Approved
OMB No. 0704-0188

1. AGENCY USE ONLY *(Leave blank)*	2. REPORT DATE	3. REPORT TYPE AND DATES COVERED
	January 2000	Final, January 1996 - March 1998

4. TITLE AND SUBTITLE
Measurement of Viscosity of Reacting Vinyl-Ester Resins Using Direct-Current Sensing

5. FUNDING NUMBERS
AH42

6. AUTHOR(S)
Bruce K. Fink, Kenric M. England,* and John W. Gillespie Jr.*

7. PERFORMING ORGANIZATION NAME(S) AND ADDRESS(ES)
U.S. Army Research Laboratory
ATTN: AMSRL-WM-MB
Aberdeen Proving Ground, MD 21005-5069

8. PERFORMING ORGANIZATION REPORT NUMBER
ARL-TR-2149

9. SPONSORING/MONITORING AGENCY NAMES(S) AND ADDRESS(ES)

10.SPONSORING/MONITORING AGENCY REPORT NUMBER

11. SUPPLEMENTARY NOTES
* University of Delaware

12a. DISTRIBUTION/AVAILABILITY STATEMENT
Approved for public release; distribution is unlimited.

12b. DISTRIBUTION CODE

13. ABSTRACT *(Maximum 200 words)*

This study investigated the sensing of viscosity an gelation of reacting vinyl-ester (VE) resins using direct-current (DC) sensing technology. The resin system studied was a tetrabutylammonium acetate (TA)-doped Dow Derakane 411-C-50 VE resin. A model of the resistance of a reacting polymer liquid as a function of the geometrical parameters of the DC-sensing system and the material properties of the resin system was developed. The model inputs were conduction path length (L), conductor surface area (A), resin viscosity ((t)), concentration of TA ions (Ci), charge of TA ions (Qi), and size of TA ions. Estimates, using the theoretically determined values for the model inputs, for the resistance of the DC sensing system employed in this investigation were the same order of magnitude as the experimentally determined values. The developed model of a reacting polymer liquid was further extended to the sensing of gelation and then successfully applied to the on-line sensing of viscosity.

14. SUBJECT TERMS
SMART weave, composites, resin transfer molding, ionic conductivity

15. NUMBER OF PAGES
37

16. PRICE CODE

17. SECURITY CLASSIFICATION OF REPORT	18. SECURITY CLASSIFICATION OF THIS PAGE	19. SECURITY CLASSIFICATION OF ABSTRACT	20. LIMITATION OF ABSTRACT
UNCLASSIFIED	UNCLASSIFIED	UNCLASSIFIED	UL

INTENTIONALLY LEFT BLANK.

USER EVALUATION SHEET/CHANGE OF ADDRESS

This Laboratory undertakes a continuing effort to improve the quality of the reports it publishes. Your comments/answers to the items/questions below will aid us in our efforts.

1. ARL Report Number/Author ARL-TR-2149 (Fink) Date of Report January 2000

2. Date Report Received _____

3. Does this report satisfy a need? (Comment on purpose, related project, or other area of interest for which the report will be used.) _____

4. Specifically, how is the report being used? (Information source, design data, procedure, source of ideas, etc.) _____

5. Has the information in this report led to any quantitative savings as far as man-hours or dollars saved, operating costs avoided, or efficiencies achieved, etc? If so, please elaborate. _____

6. General Comments. What do you think should be changed to improve future reports? (Indicate changes to organization, technical content, format, etc.) _____

CURRENT ADDRESS

_____
Organization

_____
Name E-mail Name

_____
Street or P.O. Box No.

_____
City, State, Zip Code

7. If indicating a Change of Address or Address Correction, please provide the Current or Correct address above and the Old or Incorrect address below.

OLD ADDRESS

_____
Organization

_____
Name

_____
Street or P.O. Box No.

_____
City, State, Zip Code

(Remove this sheet, fold as indicated, tape closed, and mail.)

(DO NOT STAPLE)

DEPARTMENT OF THE ARMY

OFFICIAL BUSINESS

NO POSTAGE
NECESSARY
IF MAILED
IN THE
UNITED STATES

BUSINESS REPLY MAIL
FIRST CLASS PERMIT NO 0001,APG,MD

POSTAGE WILL BE PAID BY ADDRESSEE

DIRECTOR
US ARMY RESEARCH LABORATORY
ATTN AMSRL WM MB
ABERDEEN PROVING GROUND MD 21005-5069